

## A PHYSICAL MODEL OF THE INFRARED-TO-RADIO CORRELATION IN GALAXIES

G. HELOU AND M. D. BICAY

Infrared Processing and Analysis Center, 100-22, California Institute of Technology, Pasadena, CA 91125

Received 1992 January 10; accepted 1993 March 29

## ABSTRACT

We explore the implications of the infrared-radio correlation in star-forming galaxies, using a simple physical model constrained by the constant global ratio  $q$  of infrared to radio emission and by the radial falloff of this ratio in disks of galaxies. The modeling takes into account the diffusion, radiative decay, and escape of cosmic-ray electrons responsible for the synchrotron emission, and the full range of optical depths to dust-heating photons ( $\tau < 1$  to  $\tau \gg 1$ ). We introduce two assumptions: that dust-heating photons and radio-emitting cosmic-ray electrons are created in constant proportion to each other as part of the star formation activity, and that gas and magnetic field are well coupled locally, expressed as  $B \propto n^\beta$ , with  $\frac{1}{3} \leq \beta \leq \frac{2}{3}$ . We conclude that disk galaxies would maintain the observed constant ratio  $q$  under these assumptions if the disk scale height  $h_0$  and the escape scale length  $l_{\text{esc}}$  for cosmic-ray electrons followed a relation of the form  $l_{\text{esc}} \propto h_0^{1/2}$ ; the infrared-to-radio ratio will then depend very weakly on interstellar density, and therefore magnetic field strength or mean optical depth. Scale heights for each phase of the interstellar medium (ISM) are observed to vary little among disk galaxies, while a scaling like  $l_{\text{esc}} \propto h_0^{1/2}$  can be reasonably expected to apply to the disks associated with the various phases of the ISM. In support of this expectation, we propose a specific confinement scheme for cosmic-ray electrons which is consistent with the physical model, and has an escape scale length practically independent of density, but scaling with  $h_0$ . While more subtle effects may enter the picture and in the end determine the behavior of  $q$ , this treatment identifies the various terms that should contribute to the scatter in  $q$  in a simple physical picture.

*Subject headings:* infrared: galaxies — radiation mechanisms: cyclotron and synchrotron — radiation mechanisms: thermal — radio continuum: galaxies

## 1. INTRODUCTION

*IRAS* and radio continuum observations of star-forming galaxies have revealed a very close connection between two apparently unrelated physical mechanisms: the thermal emission from dust and the synchrotron emission from cosmic-ray electrons in the interstellar magnetic field (Dickey & Salpeter 1984; Helou, Soifer, & Rowan-Robinson 1985; de Jong et al. 1985; Wunderlich, Klein, & Wielebinski 1987; Hummel et al. 1988; review by Helou 1991; see also Rickard & Harvey 1984 for pre-*IRAS* results). Unexpected as it may be, the correlation between the far-infrared (in the 40–120  $\mu\text{m}$  range) and the radio continuum (typically  $2 \text{ cm} \leq \lambda \leq 20 \text{ cm}$ ) luminosities is the tightest and most universal correlation known among global parameters of galaxies. The rms dispersion on  $q = \log Q$ ,  $Q$  being the ratio between the infrared and radio fluxes, is  $\sim 0.18 \simeq \log(1.5)$  for all systems that derive the luminosities in question from on-going star formation, including ellipticals with hidden star-forming disks (Wröbel 1991) and distant starburst galaxies ( $z > 0.1$  and  $L_{\text{FIR}} > 10^{11} L_\odot$ ; Hacking et al. 1989).

Most recently, Condon, Anderson, & Helou (1991a) have found that  $Q$  increases gradually away from the “standard” value (a luminosity ratio of  $\sim 5 \times 10^5$ ), as the galaxy changes from heating dominated by young stars to heating by an old stellar population. This transition is best traced by a decreasing ratio of radio to optical (and concomitantly infrared to optical) luminosity. The constant  $Q$  regime is in force for  $L_{\text{FIR}}/L_B \geq \frac{1}{3}$ , which would imply effective optical depths  $\sim 0.3$  or greater, depending on the details of the spatial distribution of stars and dust, and of the heating spectrum between blue and ultraviolet (see also O’Connell 1990 for a discussion of

optical depths of galaxies). Physical models of the correlation must therefore apply to systems with small optical depths, where the assumptions of “calorimeter theories” (Völk 1989) break down. These models may however assume the young stellar population ( $M \gtrsim 10 M_\odot$ ) to be the only relevant power source, since Condon et al. (1991) observe the tightest correlation in galaxies whose energetics are entirely dominated by this population. Xu (1990) provides additional arguments in support of this assumption.

Bicay & Helou (1990a, hereafter BH90) have shown that within the disks of nearby galaxies, the infrared emission is more spatially concentrated than the radio continuum, i.e.,  $Q$  is greater in the central regions than in the outer disk. In § 2 we summarize other work pertaining to this result and review briefly a phenomenological model based on the gradient in  $Q$ .

In § 3 we develop a physical picture—first proposed by Helou & Bicay (1990)—which incorporates the effects on the cosmic-ray population of diffusion, radiative decay, and escape, and allows an explicit derivation of the ratio  $Q$ , and of the different extents of radio and infrared disks. The only assumptions used are a direct correspondence between magnetic field strength and gas density, and a relatively constant geometry in star-forming disks. The treatment deals with systems spanning a range of optical depths and luminosities and is aimed at identifying physical parameters constrained by the constancy of  $Q$ . We find that the constraints apply in first order to scale lengths describing disk geometry and the escape of cosmic rays. We also predict that the interstellar medium density—and therefore the effective optical depth—affects  $Q$  only mildly, but determines the relative sizes of a galaxy’s infrared and radio disks. Various second-order effects are discussed

in § 4, including clumping in the interstellar medium. Our physical picture constrains the manner in which cosmic rays are confined, but does not entirely define it. A cosmic-ray confinement scheme which is consistent with the physical picture is presented in § 5 as one possible example.

## 2. THE PHENOMENOLOGICAL MODEL

The comparison of 60  $\mu\text{m}$  and 20 cm morphologies in M83 and NGC 6946 by Bicay, Helou, & Condon (1989) revealed good spatial coincidence between the peaks of emission at the two wavelengths. However, a gradual decrease in the mean value of  $Q_{60} = f_{\nu}(60 \mu\text{m})/f_{\nu}(20 \text{cm})$  was also identified, consistent with the report by Beck & Golla (1988) that for M33, M31, IC 342, and M101,  $I_{\nu}(60 \mu\text{m})/I_{\nu}(11 \text{cm})$  in the central regions is about 3 times greater than in the disk, and with the study of M33 by Rice et al. (1990). BH90 then extended the result to a sample of 25 galaxies, mostly spirals, and postulated that as a rule the infrared disks of galaxies have a shorter scale length than the radio synchrotron disks, primarily because of cosmic-ray spreading. Fitt et al. (1992) examined chopped photometric channel data from the *IRAS* mission, but could not confirm this trend in  $Q$ . More recent analysis of *IRAS* survey data using spatial resolution enhancement techniques does however confirm the BH90 results (Marsh et al., in preparation). Xu et al. (1992) find no radial gradient for  $Q$  in the Large Magellanic Cloud, probably because of its irregular nature. Substantial new data for a definitive resolution of the issue may come only with the launch of *ISO*. We will proceed here assuming the BH90 results.

Since the BH90 results were derived using  $f_{\nu}(60 \mu\text{m})$  rather than  $\text{FIR} \propto [2.58f_{\nu}(60 \mu\text{m}) + f_{\nu}(100 \mu\text{m})]$  (Helou et al. 1988) which yields the best correlations with the radio, they might be suspected of being just a color effect, due to the fact that galaxies are generally warmer in the central region. That suspicion is unwarranted because the gradient in the color correction  $\text{FIR}/f_{\nu}(60 \mu\text{m})$  is small compared to the  $Q_{60}$  gradient; in the three cases detailed in Table 2 of Beck & Golla (1988), the ratio  $I_{\text{FIR}}/I_{11 \text{cm}}$  still show a factor 2 difference between the “central region” and the “disk.”

In earlier work, Klein, Wielebinski, & Beck (1984) had noted a similar disparity in scale length while comparing their radio maps of M51 to Smith’s (1982) 170  $\mu\text{m}$  map: Both the thermal radio and the far-infrared disks had scale lengths of about 2.2 kpc, whereas the nonthermal radio disk fell off twice as slowly with radius. Buczylowski (1988) derived a similar result for the thermal and nonthermal radio scale lengths in M33, noting in addition that the surface density of supernova remnants fell off like the thermal disk.

BH90 derived from these observations a phenomenological model that described the radio disk as the result of spatially smearing the infrared disk by the combined effects of cosmic-ray spreading, escape, and decay. The two basic assumptions were a tight coupling between the origins of dust-heating radiation and of radio-emitting cosmic-ray electrons, and a steady-state star formation activity in the disk on kiloparsec scales. The observational constraints were the radio maps and the  $Q$  gradients. This phenomenology described adequately the large-scale disk properties, with the following results: (1) Gaussian smearing functions yield excessively broad radio disks, suggesting that additional processes besides random-walk diffusion must affect cosmic-ray evolution; (2) an exponential smearing function of the form  $I(r) = I_0 e^{-r/r_0}$  provides

better fits to the data; and (3) typical scale lengths  $r_0$  in the galaxies modeled are in the range 1–5 kpc.

At first sight, this behavior within galaxy disks appears to widen the gap between radio and infrared luminosities, by adding a spatial disparity to the difference in emission mechanisms. However, by ruling out local regulation of  $Q$ , this behavior points out the importance of the coupling between the sources and luminosities of cosmic rays on one hand, and dust-heating photons on the other. This suggests that the constancy of global  $Q$  derives from the manner in which a galaxy filters the luminosities deposited into it by star-formation activity.

## 3. THE PHYSICAL PICTURE

We propose a simple treatment of the physics pertaining to  $Q$  in the case of a disk galaxy whose star-formation rate and optical depth to the heating radiation are free parameters. In what follows we will introduce the representation of the galaxy, then evaluate  $Q$  for the system in terms of its physical parameters, and write down the two conditions equivalent to  $Q = \text{constant}$  (eqs. [6a] and [6b]). One of the conditions (eq. [6a]) will lead naturally to an assumption linking the production rates of cosmic rays and heating photons (§ 3.1); the other condition (eq. [6b]) will be met by introducing another assumption linking gas density and magnetic field strength (§ 3.2). We will then summarize the physical model and demonstrate that the two assumptions do result in  $Q = \text{constant}$  under reasonable conditions (§ 3.3).

Let us assume a “single population” galaxy in steady state (see § 3.4 for a definition), where the heating of the dust and the generation of cosmic rays are linked only to young stars. This simplification is based on strong evidence associating the constancy of  $Q$  exclusively with the young stellar population (Condon et al. 1991a). Stars as an energy source can then be characterized by two time-independent quantities, the dust-heating luminosity  $L_{\text{heat}}$ , and the luminosity in cosmic-ray electrons  $L_{\text{CR}}$ . We also adopt a simple geometry for gas and dust, representing their distribution by a disk whose density is uniform in the horizontal plane, and falls exponentially in the vertical direction.

We start by writing down the total infrared luminosity emerging from a galaxy  $L_{\text{FIR}}$  in terms of  $L_{\text{heat}}$ , the rate at which heating photons are supplied to the interstellar medium, and  $\bar{\tau}$ , a representative optical thickness of the dust to the heating radiation. Both  $L_{\text{FIR}}$  and  $\bar{\tau}$  are defined by

$$L_{\text{FIR}} \equiv L_{\text{heat}}(1 - e^{-\bar{\tau}}) \equiv L_{\text{heat}} \langle 1 - e^{-X_d n_H h_H} \rangle \quad (1)$$

where  $n_H$  and  $h_H$  represent the effective density and path length through the interstellar medium (ISM) for each line of sight, and  $X_d$  scales the exponent to an optical depth, and includes a dust-to-gas ratio; the angular brackets denote an average taken over all directions of lines of sight originating in a star. For heating sources in the midplane of a horizontally infinite uniform disk, the average can be well represented by the approximation  $\tau \simeq (2.3X_d n_0 h_0)^{0.77}$ , where  $n_0$  and  $h_0$  are the midplane density and the scale height of the interstellar gas. This approximation holds for  $\bar{\tau}$  in the range 0.03–10, which is amply sufficient for our purposes. A similar approximation, with an exponent of 0.90 was derived by Xu & de Zotti (1989) for the case of a mixed population of dust and heating sources, both exponentially distributed in the vertical direction. We therefore adopt for equation (1) the general form of equation

(2), and introduce  $\tau_0$  using the definition:

$$\begin{aligned} L_{\text{FIR}} &= L_{\text{heat}} \{1 - \exp[-(gX_d n_0 h_0)^a]\} \\ &\equiv L_{\text{heat}} [1 - \exp(-\tau_0^a)], \end{aligned} \quad (2)$$

where  $g \sim 2$  and  $a \sim 0.8$  vary slowly with geometry and with the relative distribution of dust and stars. Using the standard ratio  $A_V/N_H = 5.3 \times 10^{-22} \text{ mag cm}^2$  (Bohlin, Savage, & Drake 1978), we find  $\tau_0 \simeq (n_0/1 \text{ cm}^{-3})(h_0/100 \text{ pc})$  for the absorption in the range 1000–2000 Å, about 3 times greater than at  $V$  (5500 Å).

The emerging synchrotron luminosity  $L_{\text{sync}}$  on the other hand can be expressed in terms of  $L_{\text{CR}}$ , the rate at which energy in the form of cosmic-ray electrons is generated. Neglecting adiabatic losses and assuming that inverse Compton and synchrotron losses maintain the same ratio in disk galaxies (more about this assumption in § 4.2 below),  $L_{\text{sync}}$  is simply proportional to  $L_{\text{CR}}$  reduced by the rate at which cosmic-ray electrons escape from the galaxy. Characterizing  $L_{\text{CR}}$  by a typical electron energy, its time evolution is dominated by synchrotron losses until its escape from the galaxy. This typical-electron approximation for  $L_{\text{CR}}$  is valid since the energy spectrum of cosmic-ray electrons, or equivalently the synchrotron emission spectrum, is similar among galaxies (Klein 1990). If the typical electron is injected with energy  $E_0$  and escapes with energy  $E_{\text{esc}}$ , we write

$$L_{\text{sync}} = \chi L_{\text{CR}} \left(1 - \frac{E_{\text{esc}}}{E_0}\right). \quad (3)$$

The constant of proportionality  $\chi$  is the fraction of their energy that cosmic-ray electrons resident in a galaxy lose as synchrotron radiation, as opposed to inverse Compton or other losses. In a uniform magnetic field  $B$ , an electron's energy decays with time  $t$  as  $(1 + t/t_{\text{sync}})^{-1}$ , where  $t_{\text{sync}}$  is the lifetime of a cosmic-ray electron against synchrotron losses (Salter & Brown 1988):

$$t_{\text{sync}} \simeq 8 \times 10^9 \text{ yr} (\sin \Psi)^{-2} \left(\frac{\bar{B}}{1 \mu\text{G}}\right)^{-2} \left(\frac{E_0}{1 \text{ GeV}}\right)^{-1}, \quad (4)$$

where  $\Psi$  is the angle between the cosmic ray's momentum vector and  $B$ , and  $\bar{B} = \frac{2}{3}B_0$  is the emissivity-weighted mean field strength. Calling  $t_{\text{esc}}$  the typical time before escape, and using the definition  $t_x \equiv t_{\text{esc}}/t_{\text{sync}}$ , equation (3) becomes

$$L_{\text{sync}} = \chi L_{\text{CR}} \left(\frac{t_x}{1 + t_x}\right). \quad (5)$$

In order to maintain a constant  $L_{\text{FIR}}/L_{\text{sync}}$  ratio in the presence of luminosity and optical depth variations, galaxies obeying equations (2) and (5) have to maintain both  $L_{\text{heat}}/L_{\text{CR}}$  constant, and the ratio of  $1 - \exp(-\tau_0^a)$  to  $t_x(1 + t_x)^{-1}$  constant for any value of  $t_x$  or  $\tau_0$ . It turns out that this last ratio  $R_d(\tau)$  is a weak function of  $\tau$  for values of  $a$  and  $\tau$  in the range of interest, when  $t_x \equiv \tau_0 \equiv \tau$ . As illustrated in Figure 1 (*solid lines*), the ratio remains in the range 1–1.5 for  $\tau > 0.1$  and  $a \geq 0.8$ , and approaches 1 for large values of  $\tau$ . We therefore conclude that the observed constancy in the global infrared-to-radio ratio obtains from the combination of conditions

$$\frac{L_{\text{heat}}}{L_{\text{CR}}} = \text{constant}, \quad (6a)$$

and

$$t_x = \tau_0, \quad (6b)$$

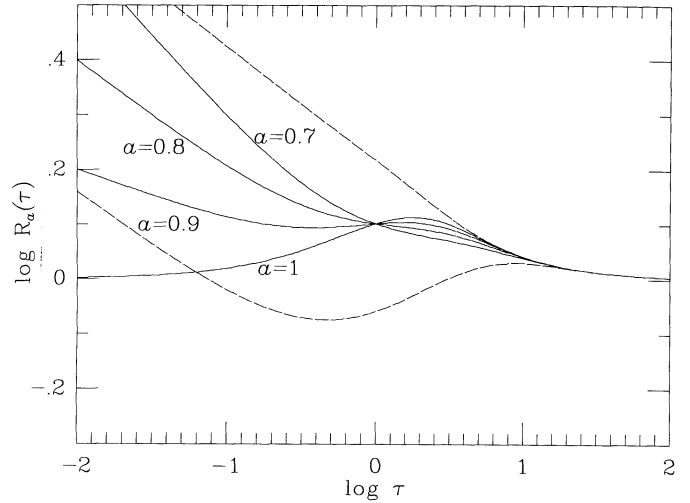


FIG. 1.—The ordinate  $R_d(\tau) = [1 - \exp(-\tau_0^a)]/[t_x(1 + t_x)^{-1}]$  is the ratio of effective optical depths of the galaxy to optical radiation and cosmic-ray electrons. The solid lines show the behavior for various values of  $a$  for  $\tau = t_x$ , as discussed in § 3. The dashed lines represent the value that would be assumed by  $R_{0.8}(\tau)$  for each of the cases  $\tau = 0.5t_x$ , and  $\tau = 2t_x$ .

with condition (6b) relaxing to both  $t_x > 5$  and  $\tau_0 > 5$  for optically thick systems. In the two subsections which follow, we discuss the implications of each of the two conditions above, then summarize the resulting physical picture in § 3.3 below.

### 3.1. Luminosities

A connection between  $L_{\text{heat}}$  and  $L_{\text{CR}}$  is a reasonable expectation once star-formation activity is accepted as the source of both luminosities (Harwit & Pacini 1975; Helou et al. 1985; Condon et al. 1991a). The condition of a constant ratio  $L_{\text{heat}}/L_{\text{CR}}$  however ties cosmic-ray acceleration more narrowly to the young stellar population, e.g., to supernova events or the termination shocks of stellar winds emanating from massive stars (Duric 1988). Moreover, to the extent that  $L_{\text{heat}}$  and  $L_{\text{CR}}$  are differently weighted integrals over the initial mass function (Condon 1992), their proportionality constrains variations in this function among galaxies. The numerical values of  $Q$  entails  $L_{\text{heat}} \simeq 5 \times 10^5 L_{\text{CR}}$ , which translates into a constraint on the efficiency of cosmic-ray production by massive stars. Since the energy density in all cosmic rays is estimated to be 30–100 times greater than that of the electron component alone (Bloemen 1989), and since the electrons will decay both by inverse Compton and synchrotron processes, that efficiency may amount at most to  $\sim 10^{-3}$  of the heating luminosity. Condition (6a) can thus be met without imposing severe requirements on the energetics of stars.

### 3.2. Optical Depths

It is less intuitive how the equality  $t_x = \tau_0$  would come about. To explore its consequences in relation to the physics and structure of the interstellar medium, we introduce the assumption that the magnetic field and the gas are well coupled locally, expressed as

$$\frac{B}{B_1} = \left(\frac{n}{1 \text{ cm}^{-3}}\right)^\beta, \quad \frac{1}{3} \leq \beta \leq \frac{2}{3}. \quad (7)$$

While the data within the Milky Way at densities greater than  $\sim 10 \text{ cm}^{-3}$  (e.g., Fiebig & Güsten 1989) agree well with this assumption, supporting evidence is much harder to obtain for lower densities, or for comparison among galaxies. We adopt

$B_1 = 5 \mu\text{G}$ , in agreement with estimates derived from observations of galaxies and of the Milky Way (Beck 1991; Condon 1992).

The escape time scale in the numerator of  $t_x$  may be written in terms of interstellar medium parameters under the assumption that individual cosmic rays travel by random walk diffusion before they escape the disk of the galaxy. If the total distance traveled radially from the point of origin is  $l_{\text{esc}}$ , and the mean free path is  $l_{\text{mfp}}$ , then the time to escape for a relativistic electron is on average (e.g., Chandrasekhar 1943)

$$t_{\text{esc}} \simeq 10^7 \text{ yr } (\cos \Psi)^{-1} \left( \frac{l_{\text{mfp}}}{1 \text{ pc}} \right)^{-1} \left( \frac{l_{\text{esc}}}{1 \text{ kpc}} \right)^2. \quad (8)$$

If diffusion was isotropic, and cosmic-ray electrons escaped unimpeded upon reaching a certain height above the disk, then  $l_{\text{esc}}$  cannot exceed the thickness of the disk. One observes however a diffuse synchrotron disk (BH90 and § 2 above), which suggests values of  $l_{\text{esc}}$  in the range  $\gtrsim 1 \text{ kpc}$ , a full order of magnitude larger than the scale heights of the molecular or atomic disks, and comparable to or slightly larger than the scale heights of the radio disks (§ 4.4 below). While improved estimates of  $l_{\text{esc}}$  are needed, the data now available force us to one of two possibilities, either highly anisotropic diffusion, or vertical confinement to delay escape and allow horizontal spreading. These two scenarios are discussed in more detail below (§ 5), resulting in the preference for the second one. For the purposes of this section however, we need only point out that either scenario may be approximated as three-dimensional diffusion projected onto a median plane. Equation (8) represents this by setting  $l_{\text{esc}}$  to half the distance diffused in a three-dimensional random walk. Since the most likely diffusion mechanism is the scattering of cosmic rays off local perturbations in the magnetic field, we write

$$l_{\text{mfp}} = 1 \text{ pc} \left( \frac{E_0}{10 \text{ GeV}} \right)^\eta \left( \frac{n_0}{1 \text{ cm}^{-3}} \right)^{-1/3}, \quad (9)$$

where the coefficient  $\eta$  depends on the spatial correlation function of the field  $B$  and is most probably between 0.5 and 1 (e.g., Cesarsky 1980). Using emissivity-weighted means  $\bar{E}$  and  $\bar{n}$  in equation (9) does not change the numerical coefficient significantly because it turns out that  $\bar{E}^{0.75} \bar{n}^{-1/3} \approx E_0^{0.75} n_0^{-1/3}$ . The exponent of  $n_0$  in equation (9) assumes that the cosmic-ray scattering is dominated by localized significant  $B$  perturbations, whose spatial density is proportional to the density of the gas. If the scattering is instead dominated by the cumulative effect of slight variations in  $B$ , and if  $B$  scales in a self-similar fashion as  $n$  varies, then the exponent of  $n$  in equation (9) would be  $-\beta - \frac{1}{3}$ .

Combining equations (8) and (9), using equation (4) for the decay time associated with synchrotron losses for a single electron, and averaging over pitch angle, we get

$$t_x \equiv \frac{t_{\text{esc}}}{t_{\text{sync}}} = 0.25 \left( \frac{n}{1 \text{ cm}^{-3}} \right)^{2\beta+1/3} \left( \frac{E_0}{10 \text{ GeV}} \right)^{1-\eta} \left( \frac{l_{\text{esc}}}{1 \text{ kpc}} \right)^2, \quad (10)$$

which is a measure of the effectiveness of a galactic disk at extracting radio emission from the cosmic-ray electron before it escapes. For either one of the diffusion or confinement scenarios sketched above, the distribution of  $l_{\text{esc}}$  will approach a modified Gaussian with a mean much larger than the dispersion, thus allowing the system to be characterized

by a ‘‘typical’’  $l_{\text{esc}}$ . Equating the expression for  $t_x$  in equation (10) to  $\tau_0$  as derived above following equation (2),  $\tau_0 \simeq (n_0/1 \text{ cm}^{-3})(h_0/100 \text{ pc})$ , yields the condition

$$\left( \frac{l_{\text{esc}}}{1 \text{ kpc}} \right) = 2 \left( \frac{E_0}{10 \text{ GeV}} \right)^{(\eta-1)/2} \left( \frac{n_0}{1 \text{ cm}^{-3}} \right)^{(1/3)-\beta} \left( \frac{h_0}{100 \text{ pc}} \right)^{1/2}. \quad (11)$$

The weak dependence on  $E_0$  would disappear altogether if one adopts  $\eta = 1$ . Since the observations typically concentrate on a given radio frequency, they select in effect just those cosmic-ray electrons with the right injection energy to yield the observed synchrotron frequency in the prevailing magnetic field. Thus for radio observations at 1.4 GHz, one may replace  $(\bar{E}/10 \text{ GeV})$  by  $(\bar{B}/1 \mu\text{G})^{-1/2}$ , or equivalently,  $(E_0/10 \text{ GeV})$  by  $2(B_0/1 \mu\text{G})^{-1/2}$  in equation (11) to obtain

$$\left( \frac{l_{\text{esc}}}{2 \text{ kpc}} \right) \left( \frac{h_0}{100 \text{ pc}} \right)^{-1/2} \left( \frac{n_0}{1 \text{ cm}^{-3}} \right)^{-\epsilon} = 1, \quad -\frac{1}{3} \leq \epsilon \leq \frac{1}{24}, \quad (12)$$

### 3.3. Interpretation

To summarize, the physical model for the radio-infrared correlation has at its base the tight coupling between the dust-heating photon luminosity  $L_{\text{heat}}$  and the production rate  $L_{\text{CR}}$  of radio-emitting cosmic-ray electrons. These two luminosities are reprocessed differently by the galaxy, with filters characterized by parameters  $t_x$  and  $\tau_0$ ;  $t_x$  determines the efficiency with which the galaxy extracts synchrotron radiation from the cosmic rays before the escape, and  $\tau_0$  represents an effective optical depth to the dust heating luminosity. The model postulates that the condition  $t_x = \tau_0$  prevails in normal galaxies, and distinguishes between two regimes. The optically thick or ‘‘calorimeter’’ regime applies to infrared-luminous galaxies which have values of  $t_x$  and  $\tau_0$  large compared to one, and thus convert all of  $L_{\text{CR}}$  and  $L_{\text{heat}}$  into radio and infrared radiation. On the other hand, the optically thin regime concerns most normal galaxies whose  $t_x = \tau_0$  ranges from  $\sim 10^{-1}$  up to a few; these systems extract roughly equal fractions of both  $L_{\text{CR}}$  and  $L_{\text{heat}}$  to yield a constant overall  $Q$ , with the balance of  $L_{\text{CR}}$  and  $L_{\text{heat}}$  escaping. In the linear approximation, the extracted fraction would come to  $t_x = \tau_0$ ; since  $\tau_0$  scales like the gas density  $n$ , and  $t_x$  scales like  $B^2$  (in the typical-electron approximation), a relation of the form  $B \propto n^{1/2}$  would result in  $t_x = \tau_0$ . Thus the assumption of a tight coupling between  $B$  and  $n$  as expressed in equation (7) is an essential element of the model.

More rigorously, the combination of the  $B$  and  $n$  coupling in equation (7) and the condition  $t_x = \tau_0$  in equation (6b) yield equation (12), which relates to the midplane gas density, the scale height of the gas disk, and the escape scale length of cosmic-ray electrons. An important feature of condition (12) is its weak dependence on density through the power index  $\epsilon = (1/3) - (3\beta/4) - (\eta\beta/4)$ . The range in  $\epsilon$  shown in equation (12) reflects both the range in  $\beta$  (coupling index between  $n$  and  $B$ ), and the range in  $\eta$  (scaling index between cosmic-ray mean free path and energy). Equation (12) may therefore be interpreted to mean that a sufficient condition for constant  $Q$  is that  $l_{\text{esc}}$  be roughly constant among galaxies, regardless of their mean interstellar density.

This result can be extended from a single-disk galaxy to one whose gas is distributed in a linear combination of a few disks

accounting for different phases of the ISM, e.g., the molecular material, the thin H I layer, the warm H I, and the ionized gas layer. These disks have  $h_0$  ranging from 100 pc to 1 kpc within the same galaxy, but remaining relatively constant for the same phase among galaxies. Different galaxies may have varying fractions of their ISM mass in the different phases, with the total  $n_0$  ranging from near 0.1 to about  $20 \text{ cm}^{-3}$  for “normal” galaxies. For the result to hold in a natural way, the condition in equation (12) needs to be satisfied for each of the disks in the same galaxy, leading to the same ratio  $Q$  for each phase. This in turn leads to the same ratio  $Q$  for the whole system, regardless of the fraction of the ISM in each phase. This suggests the interpretation of equation (12) as a scaling law of the form  $l_{\text{esc}} \propto h_0^{1/2}$ , a quite reasonable expectation for the behavior of cosmic-ray electrons in disks of different thicknesses. We discuss scale heights of  $n_0$  and  $B$  in § 4.4 and revisit this interpretation in § 5 below.

The physical picture developed above does not include any free parameters. It is therefore gratifying to find condition (12) constraining the physical parameters to values that correspond closely to what is actually observed. In particular, for  $100 \text{ pc} \leq h_0 \leq 1 \text{ kpc}$ ,  $l_{\text{esc}}$  needs to be on the order of a few kpc, precisely the range covered by  $r_0$  the scale length of the smearing function (§ 2). Since the smearing function is a combination of escape and decay,  $r_0$  must be to first order the smaller of  $l_{\text{esc}}$  and  $l_{\text{sync}}$ , defined as the distance diffused in  $t_{\text{sync}}$ . Figure 2 shows the estimated time scales and scale lengths for escape and for synchrotron decay as a function of interstellar gas density  $n_0$  in the galaxy disk with  $h_0 = 100 \text{ pc}$ , for  $\beta = \frac{1}{2}$  and  $\eta = 1$ . In galaxies with  $n_0 \lesssim 1 \text{ cm}^{-3}$ , cosmic-ray electrons escape before the onset of substantial synchrotron losses, so that  $r_0 \simeq l_{\text{esc}}$ . As  $n_0$  and  $B_0$  increase, radiative losses begin to dictate the value of  $r_0$ , eventually bringing it down to  $\lesssim 1 \text{ kpc}$  for  $n_0 \sim 20 \text{ cm}^{-3}$ . We thus predict for these denser systems that the radio and infrared disks become more similar. Condon et al. (1991b) have discussed similar physics extending the present discussion to high-density, compact, ultraluminous starbursts.

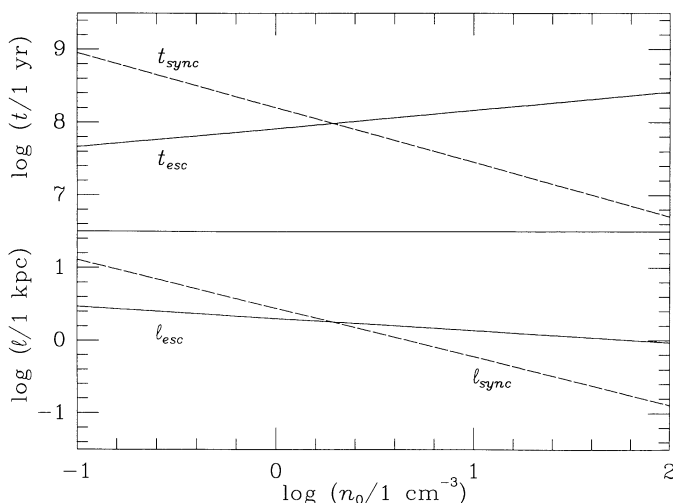


FIG. 2.—The upper panel shows the escape and synchrotron decay time scales as a function of mean interstellar density varying from 0.1 to  $100 \text{ cm}^{-3}$ , in a disk model where  $h_0 = 100 \text{ pc}$ ,  $B/1 \mu\text{G} = (n/1 \text{ cm}^{-3})^{1/2}$ , and  $l_{\text{mfp}} = 1 \text{ pc} \times (E_0/10 \text{ GeV})(n/1 \text{ cm}^{-3})^{-1/3}$ . The lower panel shows the behavior of the escape and synchrotron decay scale lengths for the mean density of the same model disk varying from 0.1 to  $100 \text{ cm}^{-3}$ . See § 3.3 for more details.

### 3.4. Time Scales

The time scales in Figure 2 also dictate the definition of the “steady state” assumption in describing the star-formation activity. In this physical picture, star formation needs to be sustained for periods on the order of a hundred million years in systems with  $n_0 \sim 1 \text{ cm}^{-3}$ , but for shorter periods in denser systems, e.g., only  $2 \times 10^7 \text{ yr}$  at  $n_0 \sim 20 \text{ cm}^{-3}$ .

Radio emission associated with local, transient bursts of star formation outlines a relativistic electron cloud that has not yet diffused to its escape or decay size. For instance during the first  $10^6 \text{ yr}$  after such a burst in a disk with  $n_0 \sim 1 \text{ cm}^{-3}$ , the radio emission patch will grow to just a few hundred parsecs in size, somewhat larger than the infrared patch. The observed ratio  $Q$ , however, will be unusually high in this patch, since the massive stars will be delivering their dust-heating luminosity into the disk, whereas the cosmic-ray electrons will still be far short of their radiative decay time scale  $t_{\text{sync}}$ . It is by averaging over many star-formation sites and life cycles that the mean  $Q$  for the galaxy is achieved.

## 4. DISCUSSION

The derivations above identify two assumptions (eqs. [6a] and [7]) and a condition (eq. [12]) which are sufficient to ensure that the global ratio of infrared to radio synchrotron luminosities is constant and equal to the observed value. The physical picture underlying these derivations reproduces the correct scale length of the large-scale variation of the infrared-to-radio within disks. We should note that a theory for the regulation of the infrared-to-radio ratio which included escape of cosmic rays and invoked equipartition of energy was proposed by Chi & Wolfendale (1990). That theory however resulted in a nonlinear relation between the infrared and radio luminosities, which has been recently proved to be a misinterpretation of the data (Condon et al. 1991a).

One test of this physical picture is severity of the constraints that need to be imposed on the physical parameters of disk galaxies in order to obtain the observed radio-infrared correlation. Formally, the slope allowed in these constraints is dictated by the 50% rms dispersion on the infrared-to-radio ratio. The dispersion on  $Q$  (0.2 on a log scale) scales to a factor 2 dispersion allowed on the condition  $t_x = \tau_0$  (eq. [6b]), for values of  $\tau \geq 0.3$ , as illustrated in Figure 1 (dashed lines). Since the expression on the left-hand side of equation (12) corresponds to  $(t_x/\tau_0)^{1/2}$ , the allowed dispersion on the expression is  $2^{1/2} \sim 40\%$ . For midrange choices of  $\beta$  and  $\eta$ , one has  $\epsilon = -0.135$ ; the full range of variation in  $n_0$  (a factor of 20) raised to this power can still be tolerated. On the other hand, the  $2^{1/2}$  constraint on  $l_{\text{esc}} h_0^{-1/2}$  demonstrates the importance of the cosmic-ray confinement mechanism which couples the escape scale length and the disk thickness:  $l_{\text{esc}}$  must be constant to within 40% for a given  $h_0$ , and the scaling must hold over roughly one order of magnitude in  $h_0$  (100 pc to 1 kpc). While the specific confinement scheme we discuss in § 5 does provide such a coupling, it yields a scaling law sufficiently different ( $l_{\text{esc}} \propto h_0$ ) that it would not meet the constraints over the full range expected for  $h_0$ . The more essential element illustrated in § 5 is the possibility of devising natural confinement schemes which yield escape scale lengths largely independent of the density of the medium.

The other significant constraint required by this physical picture is the coupling between interstellar gas density and magnetic field strength (eq. [7]). In the linear approximation,

equation (7) is also equivalent to  $(t_x/\tau_0)^{1/2} = 1$ , so the value of  $B$  is constrained to the  $2^{1/2}$  margins for a given  $n$ . This constraint is not however, unreasonable, since it needs to apply only to the mean  $B$  and  $n$  over the smallest scales relevant to the synchrotron or infrared emission mechanisms, typically 100 pc for  $n_0 \simeq 1 \text{ cm}^{-2}$ . In addition, the exact value of the exponent  $\beta$  in equation (7) is not critical, as long as it is between  $\frac{1}{3}$  and  $\frac{2}{3}$ . The physical model should remain valid even if  $\beta$  varied slowly with density, e.g., assuming smaller values at lower densities as the data in Fiebig & Güsten (1989) might suggest.

In the following subsections, we discuss clumping and inverse Compton losses as potential additional sources of dispersion on  $Q$  and revisit other assumptions.

#### 4.1. Clumping

We have implicitly assumed that the coupling between gas density and magnetic field strength holds in the mean among galaxies, as well as on all spatial scales and for all densities contributing significantly to the emission within a galaxy. The latter aspect of the assumption is well justified by the data in Fiebig & Güsten (1989). However, if the ratio of radio-to-infrared emissivity had a strong density dependence, then density fluctuations within a galaxy could introduce substantial departures from the balanced picture of a “uniform” medium discussed in § 3 above. In order to assess the importance of clumping on our results, we examine the manner in which the density variations in the medium are sampled by the two emission mechanisms. The infrared emissivity of an optically thin segment of the interstellar medium is determined by the heating flux crossing it  $\Phi_{\text{heat}}$  and the total optical depth through it; using the notation of equation (1),

$$\Lambda_{\text{IR}} \propto \Phi_{\text{heat}} \int n_{\text{H}} dl. \quad (3)$$

On the other hand, the synchrotron emissivity in the same limit would depend on the strength of the magnetic field, and the amount of time cosmic rays spend at each location. For a population of relativistic electrons with an energy distribution  $N(E) \propto E^{-2.6}$  (Condon 1992), one can write

$$\Lambda_{\text{sync}} \propto \int N_{\text{CR}} B^{3.6/2} \frac{dt}{dl} dl \propto \langle N_{\text{CR}} \rangle \int B^{3.6/2} \frac{dl}{v_{\text{eff}}}, \quad (14)$$

where  $\langle N_{\text{CR}} \rangle$  is the mean density for the galaxy as a whole. The effective velocity at which the cosmic rays diffuse through the medium is inversely proportional locally to the mean free path  $l_{\text{mfp}}$ . Using equations (7) and (9), one obtains

$$\begin{aligned} \Lambda_{\text{sync}} &\propto \langle N_{\text{CR}} \rangle \int B^{3.6/2} n^{1/3} dl \\ &\propto \langle N_{\text{CR}} \rangle \int n^{1+\alpha} dl, \quad \frac{-1}{15} \leq \alpha \leq \frac{8}{15}. \end{aligned} \quad (15)$$

The interstellar density enters the kernel of both emissivity integrals with a power close to one. Clumping will not therefore induce serious departures from proportionality between the two emission mechanisms, as long as both heating photons and cosmic-ray electrons explore the medium equally unimpeded. This exploration may fail if, for instance, the magnetic field impedes the progress of cosmic rays into denser regions by

mechanisms that are not accounted for in the simple diffusion treatment.

#### 4.2. Inverse Compton Losses

In § 3, we simply assumed that synchrotron and inverse Compton losses would occur in constant ratio to each other and limited the radiative decay treatment to the first mechanism. The ratio is given simply by the ratio of magnetic field energy density to photon energy density, and is not a priori guaranteed to be constant. Völk (1989), however, estimates this ratio to be the same in the Milky Way and M82, with a value between  $\frac{1}{3}$  and  $\frac{1}{2}$ , and postulates it to be constant among star-forming galaxies. Independently, Parravano (1988) has argued that star formation is self-regulated by feedback between the UV energy density and the critical pressure for cloud condensation out of the warm interstellar gas: an enhanced radiation field mitigates condensation and eventually star formation, while the latter can proceed more easily in a reduced radiation field. In a similar vein, Beck (1991) has suggested that the star-formation rate could be a function of the magnetic field strength, again causing a link between the magnetic energy density and the radiation energy density. Regardless of the detail, such feed-back loops would lead galaxies to keep their magnetic, gas-kinetic, and radiation pressures—and energy densities—comparable, a situation that obtains in our Galaxy, and has long been deemed necessary for equilibrium in general (Spitzer 1978).

#### 4.3. Magnetic Field

The  $\beta$  range assumed in § 3 corresponds, besides observations, to theoretical expectations from the various mechanisms that could underlie the coupling expressed in equation (7). The most likely coupling mechanisms are static pressure equilibrium between the magnetic field and the gas (Kulkarni & Heiles 1990), or equipartition between the magnetic field energy density and the turbulent kinetic energy density, mediated by dynamo effects which sustain the magnetic field in the turbulent medium (Ruzmaikin, Sokoloff, & Shukurov 1988; Ko & Parker 1989). In either case, the balance is between  $B^2$  and  $n$ , and therefore  $\beta = \frac{1}{2}$ .

For each of the mechanisms above, one is forced eventually to consider the physical link between magnetic field and gas, which is based on the charge density. In the neutral or nearly neutral medium responsible for most of the infrared emission, the charge is provided mostly by metallic ions rather than  $\text{H}^+$ . Thus the relation in equation (7) may in reality involve metallicity in a fashion that balances the term  $X_d$  in equation (1), in effect removing metallicity as an additional free parameter that may cause variations in the infrared-to-radio ratio.

#### 4.4. Scale Heights

The assumption of well-coupled gas and magnetic field (eq. [7]) implies that the  $B$  distribution is tied to the gas distribution. For the geometry we have adopted, and for a gas density scale height  $h_0$ , the magnetic field strength will fall off exponentially away from the midplane of the disk with a scale height  $h_0/\beta \simeq 2h_0$ . Synchrotron emissivity varies roughly like  $N_{\text{CR}} B^2$ , with  $1.5 \leq \chi \leq 2$ . Applying the result in § 4.1 to a steady-state population of escaping electrons,  $N_{\text{CR}}$  falls off like  $n^{1/3}$ , leading to a synchrotron scale height in the range  $\frac{3}{4}h_0$  to  $h_0$ . Thus synchrotron emission and gas density scale heights are expected to be comparable in our model galaxies, whereas  $B$

itself would have a scale height larger by a factor of 2. This prediction is verified in NGC 891, for which Rand, Kulkarni, & Hester (1990) measure a scale height for the disk of high- $z$  warm ionized hydrogen of about 1 kpc, and Hummel, Beck, & Dahlem (1991) measure a scale height of 0.9 kpc for the synchrotron emission at 1.5 GHz.

The scale height of  $B$ ,  $h_B$ , is of course not directly observable. Our deduced value of  $\sim 2$  kpc for NGC 891 disagrees with the derivation by Hummel et al. (1991) of  $h_B \simeq 4$  kpc based on the assumption of local equipartition between the energy densities of magnetic field and cosmic rays. Such an assumption is clearly inconsistent with our physical picture. However, regardless of the precise value of  $h_B$ , a separate issue is raised by thick radio disks with scale heights  $h_{\text{radio}} \gg h_0$ . In the rest of this section we discuss the evidence for thick synchrotron disks, and possible resolutions to the issue.

Disk galaxies observed in sufficient detail usually reveal multiple components with distinct scale heights in the radio continuum, presumably associated with different phases of the interstellar medium. The best resolved example is the Milky Way, where Beuermann, Kanbach, & Berkhuisen (1985) have identified a thin disk and a thick disk in emission at 408 MHz. The thin disk provides 10% of the luminosity, and has an "equivalent height" of 200 pc, whereas the thick disk provides the balance of the luminosity with an equivalent height of 1.8 kpc. Hummel (1990) reviewed data on the radio disk thickness of spiral galaxies. Out of 13 objects without an active nucleus, he found 12 with a half-power full width of the intrinsic vertical radio profile ranging between 0.5 and 1.5 kpc. This translates to  $h_{\text{radio}}$  between 0.36 and 1.1 kpc. The exception, NGC 4631, has  $h_{\text{radio}} \simeq 2.7$  kpc, and appears to be extreme in this respect, as well as in its radio spectrum which flattens out substantially at frequencies below 1 GHz. Hummel et al. (1991) propose that either dynamo effects or wind models could explain the observed field structures, while Hummel & Dettmar (1990) conclude that this thick disk is probably caused by gravitational interaction with NGC 4656.

The more common values of  $h_{\text{radio}}$  found by Hummel are still considerably greater than  $h_0$  for molecular or atomic disks. Since we know from galaxies observed face-on that the diffuse ionized medium with a large scale height does not dominate the infrared luminosity, the disparity between  $h_{\text{radio}}$  and  $h_0$  challenges the validity of the assumed coupling  $B \propto n^\beta$ . The explanation for thick disks, especially in quiescent galaxies, may be that cosmic-ray electrons are confined to high-reaching but closed magnetic loops, anchored in the dense disk, and filling sparsely the halo. Another possible scenario is that the coupling between  $B$  and  $n$  breaks down above the disk, possibly due to magnetic field fragments or loops surviving after extraction from the disk superbubbles or galactic fountains. Their survival could be helped by fountain gas cooling and raining back onto the disk, or by intergalactic gas accreting onto the disk. These magnetic field fragments could be "illuminated" by the cosmic-ray electrons escaping from the disk, or by an additional population of electrons escaping from the central regions of the galaxy, where poloidal magnetic field structures facilitate escape, as suggested by Bica & Helou (1990b).

Clearly, radio data with finer spatial resolution are needed to improve our understanding of the vertical structure in these disks and to test the speculations. Thick radio disks point out the need to improve on one aspect of our physical model, namely the confinement of cosmic-ray electrons.

## 5. A COSMIC-RAY CONFINEMENT SCHEME

The model in § 3 led us to the requirement that the cosmic-ray escape scale length  $l_{\text{esc}}$  is roughly constant, independent of the density of the medium or of the associated mean free path. As an existence proof for such behavior, we now sketch out a plausible though simplistic mathematical model for confinement, which satisfies that requirement and is consistent with the physical picture developed above. Several physical analogs for this mathematical model may be envisaged, the simplest of which is a variation on the "leaky box model" (Cesarsky 1980).

Assume that cosmic-ray electrons diffuse isotropically from their sources and can reach the vertical "boundaries" of the disk in a relatively short time. Each time an electron visits that boundary, there is a small, constant probability of escape  $\epsilon_{\text{esc}} \ll 1$ . This may be interpreted as the probability that the magnetic field line at this point on the boundary is open to intergalactic space, or the probability that this section of the boundary is undergoing a Parker instability. Then the condition for escape is of the form

$$n_b \epsilon_{\text{esc}} \geq 1, \quad (16)$$

where  $n_b$  is the total number of visits to the boundary before escape. If the time between boundary visits is  $t_b$ , then the condition becomes

$$\frac{t_{\text{esc}}}{t_b} \epsilon_{\text{esc}} \geq 1. \quad (17)$$

To within geometric factors only,  $t_{\text{esc}}$  and  $t_b$  are the times required to diffuse  $l_{\text{esc}}$  and the vertical distance to the boundary, which is proportional to the scale height of the interstellar medium  $h_0$ . Thus the ratio of time scales in equation (17) may be replaced by the squared ratio of the corresponding scale lengths, which lead to

$$l_{\text{esc}} h_0^{-1} \epsilon_{\text{esc}}^{1/2} = \text{constant}. \quad (18)$$

Among similar systems where  $h_0$  and  $\epsilon_{\text{esc}}$  are comparable, this scheme predicts  $l_{\text{esc}}$  to be independent of mean free path, and therefore of density or magnetic field strength. Moreover, the scaling between  $h_0$  and  $l_{\text{esc}}$  is not significantly different from the scaling in equation (12), especially since the total range expected for the variation in  $h_0$  is less than an order of magnitude. If a leaky box model is taken as the physical analog of this confinement scheme, the reflecting boundaries tend to be highly efficient for small values of  $h_0$ , with  $l_{\text{esc}} \sim 1$  kpc and  $h_0 = 100$  pc requiring  $\epsilon_{\text{esc}} \lesssim 10^{-3}$ .

## 6. SUMMARY AND CONCLUSION

Galaxies manage to maintain their global infrared-to-radio ratio  $Q$  remarkably constant, given the disparity of the physical processes involved, and the potential number of free parameters. An important clue to this behavior is the systematic radial falloff of the local ratio  $Q$  within galaxy disks, which argues that  $Q$  must be regulated globally. We have characterized the variables relevant to this behavior in a simple physical picture which accounts for a globally constant but radially falling  $Q$ . We conclude that the regulation can result from the "universality" of the following three items: (1) star formation yields dust-heating photons and cosmic-ray electrons in a roughly constant ratio  $L_{\text{heat}}/L_{\text{CR}}$ ; (2) the geometry of cosmic-ray confinement has the scaling property  $l_{\text{esc}} \propto h_0^{1/2}$ ; and (3) gas

and magnetic field are well coupled on the scales of 10–100 pc, with  $B/B_1 = (n/1 \text{ cm}^{-3})^\beta$ , with  $B_1$ , and  $\frac{1}{3} \leq \beta \leq \frac{2}{3}$  constant among galaxies.

The physical picture we develop implies constraints on the behavior of cosmic-ray electrons, their diffusion, decay, and escape. Their confinement must allow for an escape scale length which does not depend on their mean free path, or therefore on the density of the interstellar medium. The observed dispersion on  $Q$ , a factor of  $\sim 2$ , constrains the product  $l_{\text{esc}} \times h_0^{-1/2}$  to less than 40% in variations. In this paper, we propose a specific mathematical model for confinement, akin to the leaky box model, which is consistent with the simple assumptions of our physical picture, and has  $l_{\text{esc}}$  independent of density.

It may well be that  $Q$  is regulated by some subtle process we have not considered here. This paper's aim is to identify explicitly the constraints needed in the simplest description of galaxy disks which are optically thin to the heating radiation, avoiding in particular unspecified feed-back mechanisms that lead to

indirect couplings between parameters (see review by Helou 1991). The radio emission clearly emerges as the more difficult term to capture and analyze. A more detailed examination of the radio and infrared data, in particular at higher spatial resolution, should lead eventually to a better characterization of the behavior of relativistic electrons, and of their origins and acceleration mechanisms.

We would like to thank F. de Curtis and Lou Shano for excellent suggestions, especially in the interpretation, and Mary Ellen Barba for help with the manuscript. Rainer Beck, our referee, contributed many significant suggestions, especially regarding the thickness of radio disks. Jim Condon and Neb Duric provided helpful discussions and comments. This research is supported through the *IRAS* Extended Mission Program by the Jet Propulsion Laboratory, California Institute of Technology, under a contract with the National Aeronautics and Space Administration.

## REFERENCES

- Beck, R. 1991, in *The Interpretation of Modern Synthesis Observation of Galaxies*, ed. N. Duric & P. Crane (ASP Conf. Ser. 18), 43
- Beck, R., & Golla, G. 1988, *A&A*, 191, L9
- Beuermann, K., Kanbach, G., & Berkhuijsen, E. M. 1985, *A&A*, 153, 17
- Bicay, M. D., & Helou, G. 1990a, *ApJ*, 362, 59 (BH90)
- . 1990b, in *Galactic and Extragalactic Magnetic Fields*, ed. R. Beck, P. P. Kronberg, & R. Wielebinski (Dordrecht: Kluwer), 237
- Bicay, M. D., Helou, G., & Condon, J. J. 1989, *ApJ*, 338, L53
- Bloemen, J. B. G. M. 1989, *ARA&A*, 27, 469
- Bohlin, R. C., Savage, B. D., & Drake, J. F. 1978, *ApJ*, 224, 132
- Buczilowski, U. R. 1988, *A&A*, 205, 29
- Cesarsky, C. J. 1980, *ARA&A*, 18, 289
- Chandrasekhar, S. 1943, *Rev. Mod. Phys.*, 15, 1
- Chi, X., & Wolfendale, A. W. 1990, *MNRAS*, 245, 101
- Condon, J. J. 1992, *ARA&A*, 30, 575
- Condon, J. J., Anderson, M. L., & Helou, G. 1991a, *ApJ*, 376, 95
- Condon, J. J., Huang, Z.-P., Yin, Q. F., & Thuan, T. X. 1991b, *ApJ*, 378, 65
- de Jong, T., Klein, U., Wielebinski, R., & Wunderlich, E. 1985, *A&A*, 147, L6
- Dickey, J. M., & Salpeter, E. E. 1984, *AJ*, 284, 461
- Duric, N. 1988, *Space Sci. Rev.*, 48, 73
- . 1991, in *The Interpretation of Modern Synthesis Observation of Galaxies*, ed. N. Duric & P. Crane (ASP Conf. Ser. 18), 17
- Fiebig, D., & Güsten, R. 1989, in *The Physics and Chemistry of Interstellar Molecular Clouds*, ed. G. Winnewisser & T. J. Armstrong (Berlin: Springer), 93
- Hacking, P., Condon, J. J., Houck, J. R., & Beichman, C. A. 1989, *ApJ*, 339, 12
- Harwit, M., & Pacini, F. 1975, *ApJ*, 200, L127
- Helou, G. 1991, in *The Interpretation of Modern Synthesis Observation of Galaxies*, ed. N. Duric & P. Crane (ASP Conf. Ser. 18), 125
- Helou, G., & Bicay, M. D. 1990, in *Windows on Galaxies*, ed. G. Fabbiano, J. S. Gallagher, & A. Renzini (Dordrecht: Kluwer), 115
- Helou, G., Khan, I., Malek, L., & Boehmer, L. 1988, *ApJS*, 68, 151
- Helou, G., Soifer, B. T., & Rowan-Robinson, M. 1985, *ApJ*, 298, L7
- Hummel, E. 1990, in *Windows on Galaxies*, ed. G. Fabbiano, J. S. Gallagher, & A. Renzini (Dordrecht: Kluwer), 141
- Hummel, E., Beck, R., & Dahlem, M. 1991, *A&A*, 248, 23
- Hummel, E., Davies, R. D., Wolstencroft, R. D., van der Hulst, J. M., & Pedlar, A. 1988, *A&A*, 199, 91
- Klein, U. 1990, in *Windows on Galaxies*, ed. G. Fabbiano, J. S. Gallagher, & A. Renzini (Dordrecht: Kluwer), 157
- Klein, U., Urbanik, M., Beck, R., & Wielebinski, R. 1983, *A&A*, 127, 177
- Klein, U., Wielebinski, R., & Beck, R. 1984, *A&A*, 135, 213
- Ko, C. M., & Parker, E. N. 1989, *ApJ*, 341, 828
- Kulkarni, S. R., & Heiles, C. 1988, in *Galactic and Extragalactic Radio Astronomy*, ed. G. L. Verschuur & K. I. Kellerman (New York: Springer), 95
- O'Connell, R. W. 1990, in *Windows on Galaxies*, ed. G. Fabbiano, J. S. Gallagher, & A. Renzini (Dordrecht: Kluwer), 39
- Rand, R. J., Kulkarni, S. R., & Hester, J. J. 1990, *ApJ*, 352, L1
- Rice, W. L., Boulanger, F., Viallefond, F., Soifer, B. T., & Freedman, W. 1990, *ApJ*, 358, 418
- Rickard, L. J., & Harvey, P. M. 1984, *AJ*, 89, 1520
- Ruzmaikin, A., Sokoloff, D., & Shukarov, A. 1988, *Nature*, 336, 341
- Salter, C. J., & Brown, R. L. 1988, in *Galactic and Extragalactic Radio Astronomy*, ed. G. L. Verschuur & K. I. Kellerman (New York: Springer), 1
- Smith, J. 1982, *ApJ*, 261, 463
- Spitzer, L., Jr. 1978, *Physical Processes in the Interstellar Medium* (New York: Wiley)
- Völk, H. J. 1989, *A&A*, 218, 67
- Wrobel, J. M. 1991, in *The Interpretation of Modern Synthesis Observation of Galaxies*, ed. N. Duric & P. Crane (ASP Conf. Ser. 18), 197
- Wunderlich, E., Klein, U., & Wielebinski, R. 1987, *A&A*, 69, 487
- Xu, C. 1990, *ApJ*, 365, L47
- Xu, C., & de Zotti, G. 1989, *A&A*, 225, 12
- Xu, C., Klein, U., Meinert, D., Wielebinski, R., & Haynes, R. F. 1992, *A&A*, 257, 47